PERGAMON

International Journal of Solids and Structures 39 (2002) 3741–3756

INTERNATIONAL JOURNAL OF SOLIDS and STRUCTURES

www.elsevier.com/locate/ijsolstr

Conditions for compaction and shear bands in a transversely isotropic material ☆

J.W. Rudnicki *

Department of Civil Engineering, R. McCormick School of Engineering and Applied Science, Northwestern University, 2145 Sheridan Road, Evanston, IL 60208-3109, USA

Received 7 August 2001; received in revised form 24 October 2001

Abstract

This paper derives conditions for localized deformation for a transversely isotropic constitutive relation intended to model the response of geological materials in the axisymmetric compression test. The analysis considers the possibility of shear bands, with dilation or compaction, and pure compaction bands. The latter are planar zones of localized pure compressive deformation (without shear) that form perpendicular to the direction of the maximum principal compressive stress. Compaction bands have been observed in porous rock in the field and in the laboratory. They are predicted to occur when the incremental tangent modulus for uniaxial deformation vanishes. The critical value of the tangent modulus E for constant lateral stress is $-9Kvr/2$, where v is the negative of the ratio of increments of lateral to axial deformation (at constant lateral stress), r is the ratio of axial to lateral stress increments causing zero axial deformation, and K is the modulus relating increments of lateral stress and deformation. The expression for the critical tangent modulus for shear band formation is more complex and depends, in addition to r, v, and K, on the shear moduli G_l and G_t, governing increments of shear in planes parallel and perpendicular to the axis of symmetry, respectively. Uncertainty about material parameters prevents a detailed comparison with observations but the results are consistent with observations of low angle shear bands (with normals less than 45° from the symmetry axis) for compressive volumetric strain ($v < 1/2$). In addition, the critical tangent modulus for such bands may be positive if G_l and G_t are small relative to K and r is around unity.

Keywords: Localization; Compaction; Shear bands; Geomaterials; Transverse isotropy

1. Introduction

The tendency of geological materials, rocks and soils, to fail by localizing shear deformation into narrow zones is well-known. Another less common, but possibly significant, mode of localized failure is a compaction band. These are thin, planar zones without evident shear in which the material is more compacted than in the surroundings. Compaction bands have been observed in an aeolian sandstone formation in

☆ IUTAM Symposium on Material Instabilities and the Effect of Microstructure, May 7–11, 2001, Austin, Texas.

* Tel.: +1-847-491-3411; fax: +1-847-491-4011.

E-mail address: jwrudn@northwestern.edu (J.W. Rudnicki).

0020-7683/02/$ - see front matter
PII: S0020-7683(02)00173-7

Utah (Mollema and Antonellini, 1996) and in a number of laboratory experiments (Olsson, 1999). A similar phenomenon has been observed in honeycomb structures (e.g., Papka and Kyriakides, 1999) and loosely packed granular aggregates (Gioia and Cuitiño, 2001). Because the porosity in the band is less than that in the surrounding adjacent material, the permeability is also lower. Recent experiments on Castlegate sandstone by Holcomb and Olsson (submitted for publication) have shown that the permeability is reduced by two orders of magnitude in the compacted regions. Consequently, compaction bands can act as barriers to fluid flow and their occurrence in highly porous formations can affect efforts to inject or withdraw fluids for a variety of applications. These include the extraction and storage of hydrocarbons for energy, injection of radioactive and chemical wastes, sequestration of carbon dioxide to mitigate adverse affects on the global climate (Wawersik et al., 2001) and aquifer management for industrial and agricultural use.

Because of the possible importance of compaction bands on fluid flow in porous formations, there is a need for a better understanding of the stress conditions and constitutive properties that lead to their formation. Olsson (1999) was the first to note that the conditions for compaction band formation could be addressed within the same framework used by Rudnicki and Rice (1975) to study the inception of shear bands. In this approach, conditions are sought for which the constitutive description of homogeneous deformation allows nonuniform deformation in a planar band as an alternative to further homogeneous deformation. Issen and Rudnicki (2000) reexamined the work of Rudnicki and Rice (1975) for the possibility of compaction bands. By incorporating a correction to the analysis of Rudnicki and Rice (1975) by Perrin and Leblond (1993), Issen and Rudnicki (2000) showed that solutions for compaction bands were possible within a range of parameters that are representative of highly porous rock. (Ottosen and Runesson (1991) had previously identified the mathematical possibility of this type of solution but did not discuss its physical significance.) More specifically, highly porous rocks tend to undergo inelastic compaction, possibly enhanced by shear, and to yield under purely hydrostatic compression stress. Predictions were strongly dependent on the details of the constitutive relation (Issen and Rudnicki, 2000, 2001) but it is possible for the onset of compaction bands to occur for stationary or rising loads. Issen and Rudnicki (2000) found that under modest restrictions on constitutive parameters, the most favorable deviatoric stress state for onset of compaction bands was axisymmetric compression.

This paper continues the line of investigation of Issen and Rudnicki (2000) by re-examining the analysis of Rudnicki (1977). He used a transversely isotropic constitutive relation to investigate the conditions for the onset of shear bands in the axisymmetric compression test (Fig. 1), the most common testing configuration for rock specimens. Specimens may be anisotropic due to layering or other fabric developed in situ.

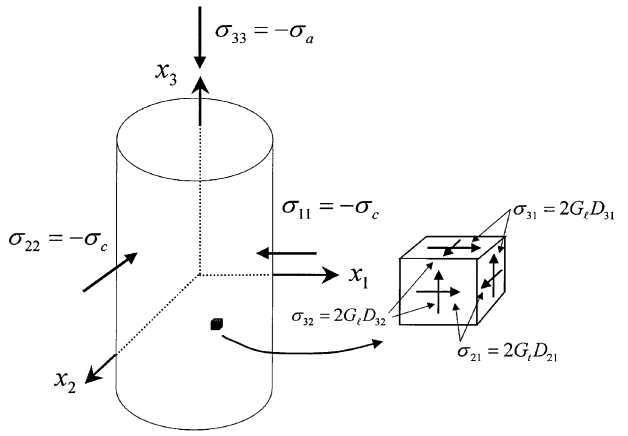

Fig. 1. Schematic illustration of the axisymmetric compression test. The x_3 axis is also the symmetry axis for transverse isotropy. Inset shows increments of shear governed by moduli G_l and G_t.

Even in specimens that are nominally isotropic before loading, the preferential growth of microcracks in the axial direction can induce a transverse anisotropy. This paper considers the possibility of compaction band formation and reexamines the conditions for shear band formation emphasizing application to highly porous rock that undergoes inelastic compaction.

2. Constitutive relation

The geometry of the axisymmetric compression test is shown in Fig. 1 and the specimen is assumed to be oriented so that the x_3 direction is the axis of symmetry. The constitutive relation used by Rudnicki (1977) (suggested by Rice, 1976 (personal communication)) is given by the following relation between the components of the rate of deformation tensor D_{ij} and the components of the Jaumann rate (Prager, 1961) of Cauchy stress $\hat{\sigma}_{ij}$

$$D_{33} = \frac{1}{E}\left\{\hat{\sigma}_{33} - r\frac{1}{2}(\hat{\sigma}_{11} + \hat{\sigma}_{22})\right\} \tag{1a}$$

$$\frac{1}{2}(D_{11} + D_{22}) = -vD_{33} + \frac{1}{9K}(\hat{\sigma}_{11} + \hat{\sigma}_{22}) \tag{1b}$$

$$D_{11} - D_{22} = \frac{1}{2G_{\mathrm{t}}}(\hat{\sigma}_{11} - \hat{\sigma}_{22}) \tag{1c}$$

$$D_{31} = \frac{1}{2G_{\mathrm{l}}}\hat{\sigma}_{31}, \quad D_{32} = \frac{1}{2G_{\mathrm{l}}}\hat{\sigma}_{32} \tag{1d}$$

For constant lateral confining pressure, $\hat{\sigma}_{11} = \hat{\sigma}_{22} = 0$, E in (1a) is the tangent modulus for axial stress versus axial strain and v in (1b) is the negative of the ratio of an increment of lateral deformation to an increment of axial deformation. The volume strain-rate, D_{kk}, is $(1 - 2v)D_{33}$ and, hence, has the same sign as D_{33} for $v < 1/2$. For axisymmetric compression ($D_{33} < 0$), the volume strain rate is compactive (typical of high porosity rock) for $v < 1/2$ and dilatant (typical of low porosity rock) for $v > 1/2$. If an increment of axial stress is accompanied by an increment of lateral confining stress $\hat{\sigma}_{11} = \hat{\sigma}_{22} \neq 0$, then r is the ratio of axial stress increment to lateral stress increment for which the axial deformation increment is zero ($D_{33} = 0$). The modulus $9K$ relates the increments of lateral deformation and stress (with $D_{33} = 0$). For isotropic elasticity and plastic normality (or a flow rule associated with the yield condition) $r = 2v$ but this condition is usually too restrictive for geological materials. Setting $D_{11} = D_{22} = 0$ (1b) and eliminating $\hat{\sigma}_{11} = \hat{\sigma}_{22}$ from (1a) reveals that $E + 9Krv/2$ is the tangent modulus for uniaxial strain. The formulation includes two shear moduli (Fig. 1). The transverse shear modulus G_{t} in (1c) governs increments of shearing transverse to the axial direction. The longitudinal shear modulus G_{l} governs increments of shearing on planes parallel to the axial direction.

Although the discussion here emphasizes the interpretation in terms of the behavior of rock, it could be applied to other materials such as metals, composites and polymers. The relation (1a)–(1d) is the most general transversely isotropic, incrementally linear form. Miles and Nuwayhid (1985) have used a constitutive relation of the same type, but written in different form, and Hutchinson and Miles (1974) used a similar relation, specialized to incompressible materials, to investigate necking bifurcations in elastic–plastic cylinders subjected to uniaxial tension. Chau (1992, 1993) used the relation (1a)–(1d) to investigate bifurcations in tension and compression of compressible elastic–plastic cylinders.

This constitutive relation can be compared with that used by Rudnicki and Rice (1975) in their shear band analysis and by Issen and Rudnicki (2000) in the analysis for the onset of compaction bands:

$$D_{ij} = C_{ijkl}\hat{\sigma}_{kl} + \frac{1}{h}\left(\frac{\sigma'_{ij}}{2\bar{\tau}} + \frac{\beta}{3}\delta_{ij}\right)\left(\frac{\sigma'_{kl}}{2\bar{\tau}} + \frac{\mu}{3}\delta_{kl}\right)\hat{\sigma}_{kl} \tag{2}$$

where C_{ijkl} is the tensor of elastic compliances, σ'_{ij} is the deviatoric stress, $\bar{\tau} = \sqrt{\sigma'_{ij}\sigma'_{ij}/2}$ is the Mises equivalent shear stress, δ_{ij} is the Kronecker delta and the second term is dropped for purely elastic deformation. The three inelastic constitutive parameters are h, β, and μ. The hardening (softening) modulus h is the slope of the shear stress versus plastic shear strain curve at constant mean stress. The dilatancy factor β is the ratio of inelastic increments of volume strain (positive in dilation) to inelastic increments of shear strain. The coefficient μ is the local slope of the yield surface in a plot of $\bar{\tau}$ versus mean compressive stress $-\sigma_{kk}/3$. A geometric interpretation of μ and β is shown in Fig. 2. For low porosity rocks (or high porosity rocks at low compressive mean stress), $\mu > 0$ and can be interpreted as a friction coefficient: further yield in shear is inhibited by increasing compressive stress. (For low porosity rocks the mean stress at which yield occurs in compression is so high that the surface is effectively open on the mean stress axis.) But, as discussed by Olsson (1999) and Issen and Rudnicki (2000, 2001) and as illustrated in Fig. 2, for high porosity rocks that yield in pure hydrostatic compression, μ will be negative as the surface approaches the hydrostatic axis.

If (2) is specialized to axisymmetric deformation and isotropic elasticity with shear modulus G_e, bulk modulus K_e and Poisson's ratio ν_e, then the parameters of (1a)–(1d) can be expressed in terms of those of (2). Both of the shear moduli in (1a)–(1d), G_t and G_l correspond to the elastic shear modulus G_e in (2). The remaining parameters of (1a)–(1d) are given terms of those of (2) as follows:

$$E \to \frac{3h}{(\delta + \beta/\sqrt{3})(\delta + \mu/\sqrt{3}) + 3h/2G_e(1+\nu_e)} \tag{3a}$$

$$r \to \frac{(\delta + \beta/\sqrt{3})(\delta - 2\mu/\sqrt{3}) + 3h\nu_e/2G_e(1+\nu_e)}{(\delta + \beta/\sqrt{3})(\delta + \mu/\sqrt{3}) + 3h/2G_e(1+\nu_e)} \tag{3b}$$

$$2v \to \frac{(\delta - 2\beta/\sqrt{3})(\delta + \mu/\sqrt{3}) + 3h\nu_e/2G_e(1+\nu_e)}{(\delta + \beta/\sqrt{3})(\delta + \mu/\sqrt{3}) + 3h/2G_e(1+\nu_e)} \tag{3c}$$

$$9K/4 \to K_e\frac{(\delta + \beta/\sqrt{3})(\delta + \mu/\sqrt{3}) + 3h/2G_e(1+\nu_e)}{1 + h/G_e + \mu\beta K_e/G_e} \tag{3d}$$

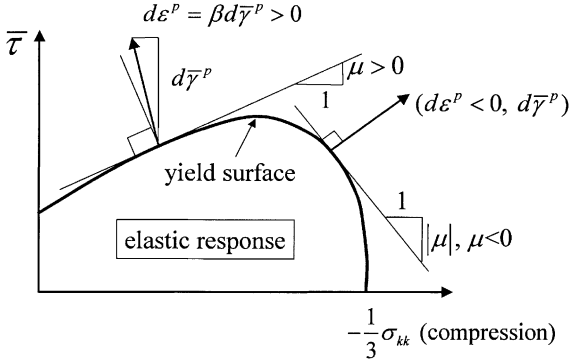

Fig. 2. Sketch of the yield surface and the inelastic strain increment vector $(d\varepsilon^p, d\bar{\gamma}^p)$ in the space of Mises equivalent shear stress $\bar{\tau}$ versus mean compressive stress $-\sigma_{kk}/3$. The slope of the surface μ and the ratio $\beta = d\varepsilon^p/d\bar{\gamma}^p$ may be positive or negative.

where $\delta = -1$ for compression and $\delta = +1$ for extension. All the constitutive parameters, including the elastic moduli, may evolve in a complex way with inelastic deformation (Holcomb and Rudnicki, 2001; Sulem et al., 1999).

3. Discussion of material parameters

Rudnicki (1977) cites values of v ranging from 0.2 to 4.1 inferred from axisymmetric compression tests on several low porosity rocks. Determining values of r requires altering the lateral stress which is not done in the conventional axisymmetric compression test. Some information can, however, be obtained from the relation (3b) and observed values of μ. For $h/G_e \ll 1$, the expression for r (3b) reduces to

$$r = (1 + 2\mu/\sqrt{3})/(1 - \mu/\sqrt{3}) \tag{4}$$

Typical values of μ for brittle, dilatant rock are in the range 0.5 to 1.0 (Rudnicki and Rice, 1975) and correspond to values of r from 2.2 to 5.1. For the same approximation, $h/G_e \ll 1$, in (3c) $2v$ reduces to

$$2v = (1 + 2\beta/\sqrt{3})/(1 - \beta/\sqrt{3}) \tag{5}$$

and values of β representative of low porosity rock, 0.2–0.5, correspond to the range 0.7–0.95 for v. For the same approximation leading to (4) and (5), E and h will have the same sign for axisymmetric compression if $\mu < \sqrt{3}$ and $\beta < \sqrt{3}$. As noted by Issen and Rudnicki (2001), the second condition must be met for axisymmetric compression deformation and violation of the first condition makes it impossible to stay on the yield surface in axisymmetric compression.

The values just cited for r and v pertain to low, porosity rock for which β and μ are positive and, typically, $\beta < \mu$. But, as noted by Olsson (1999) and Issen and Rudnicki (2000) and, as depicted in Fig. 2, both μ and β are likely to be negative for high porosity rock and sufficiently large compressive mean stress. The expressions (4) and (5) indicate that r will be positive for $\mu > -\sqrt{3}/2$ and that v will be positive if $\beta > -\sqrt{3}/2$. As the yield surface approaches the mean compression axis in Fig. 2, symmetry implies that the slope is vertical, corresponding to $\mu \to -\infty$. In this limit, r from (4) approaches -2.0. On portions of the yield surface where $\mu < 0$, the direction of the inelastic strain increment is usually assumed to be normal to the yield surface (e.g., Fossum and Fredrich, 2000; Wong et al., 1992). Hence, $\beta = \mu$ and β also becomes large and negative as the yield surface approaches the compression axis, corresponding to a limit of $v = -1$. Thus, the structure of the yield surface suggests that there will be a range of stress states near the hydrostatic compression axis where both r and v will be negative. A negative value of v means that a compressive increment of axial deformation causes a compressive increment of lateral deformation at constant lateral stress. A negative value of r means that a tensile increment of axial stress is required to maintain a zero increment of axial deformation in response to a compressive increment of lateral stress. Although anomalous, it is possible to envision this type of response for an extremely porous material with a open-cell structure but more difficult to do so for a rock with 20–30% porosity. Observational evidence is not clear since virtually all tests are either hydrostatic compression or axisymmetric compression with constant lateral stress. The load path for the latter is a line with slope $\sqrt{3}$ in the coordinates of Fig. 2. Consequently, unless the initial confining pressure is nearly the value for yield in hydrostatic compression the load path does not intersect the yield surface near the hydrostatic axis.

Direct measurement of the modulus K also requires systematic alteration of the lateral confining stress and, hence, is not well-constrained by observations. For isotropically elastic deformation $K = 4(K_e + G_e/3)/9$, but the value just prior to localization is likely much less because of damage and axial crack growth. Hoenig (1979) has made self-consistent calculations for the reduction in moduli for elastic solids

with oriented cracks. His calculations for cylindrical transverse isotropy (a random distribution of cracks with normals perpendicular to a given axis) corresponds to the axisymmetric compression geometry with cracking predominantly in the axial direction. Fig. 2 of Hoenig (1979) plots the modulus K ($\overline{E}$ in Hoenig (1979)) against a crack density parameter $\epsilon = N\langle a^3\rangle$, where N is the number of cracks per unit volume, a is the crack radius and $\langle\cdots\rangle$ denotes the orientation average. For values of ϵ equal to 0.2 and 0.4, K is reduced to about 55% and 20% of its value for the uncracked solid, respectively. These results are for flat cracks and, hence, may be more appropriate for the reductions in low porosity rock due to axial crack growth than for high porosity rocks in which the voids have more equant dimensions. Nevertheless, significant reductions in K may also be expected for high porosity rock.

The shear moduli G_t and G_l govern increments of shear superimposed upon axisymmetric loading and, hence, are also not measured in the conventional axisymmetric compression test. For a smooth yield surface elastic–plastic model, these will correspond to elastic moduli, but in rocks elastic moduli can be reduced from their initial values by cracking and other damage processes during loading. Rudnicki (1977) infers that G_l may exceed G_t by 10% from wave speed measurements on cylinders of Westerly granite (a low porosity rock) at 20 MPa (Bonner, 1974). Other indications of the reduction in the values of the shear moduli can be obtained from the self-consistent calculations of Hoenig (1979). According to the results plotted in Hoenig's Fig. 2, the modulus G_l ($\overline{G}$ in Hoenig (1979)) is reduced to about 78% and 58% of its initial value when the crack density parameter ϵ is equal to 0.2 and 0.4, respectively. The same plot shows G_t reduced to about 58% and 25% of its initial value at the same values of ϵ.

The just-cited estimates of G_t and G_l presume elastic (though, damaged) response for increments of shear as would be the case for a smooth yield surface model. Very general considerations (Hill, 1967) suggest, however, that inhomogeneous microscale processes will lead to a vertex on the yield surface at the current stress point, at least if the yield surface is defined in terms of small offset plastic strains. In this case an increment of shear superimposed upon axisymmetric deformation will cause nonelastic response. Rudnicki and Rice (1975) have suggested a model for brittle rock, similar to the slip theory of Batdorf and Budiansky (1949), that predicts vertex formation and Rudnicki and Chau (1996) have calculated the evolution of the vertex angle for torsion following axisymmetric compression for a modification of the microcrack model introduced by Costin (1983a,b). Olsson (1992) has used oscillating stress paths in a tension—compression test to infer the existence of a yield surface vertex for Tennessee marble and Olsson (1995) measured the modulus corresponding to G_l (G in his notation) in torsion tests of thin-walled cylinders of Tennessee marble (low porosity). He finds that G_l decreases approximately linearly with shear strain to about 46% of its initial elastic value at a shear strain of 0.018. Although the values of G_t and G_l corresponding to response at a vertex could, in principle, be calculated for a microstructural model, such as the self-consistent calculations of Hutchinson (1970) for polycrystalline metals, there appear to be no such calculations for geomaterials. Because of the difficulty of determining these "vertex" or out-of-plane moduli by either measurement or calculation, Vardoulakis and Graf (1985) have suggested using observations of shear band formation in granular materials to infer them. Desrues (2002) expands upon this suggestion and presents an example of its implementation for a hypo-plastic constitutive model.

4. Localization analysis

The conditions required on the velocity and stress rate fields at the inception of localization are well-established (Rice, 1976). Continuity of the velocity field requires that possible discontinuities in the velocity gradients are limited to the form

$$\Delta\left(\frac{\partial v_i}{\partial x_j}\right) = n_j g_i \tag{6}$$

where Δ is the difference between $(\cdots)$ inside and outside of the band, the n_i are components of the unit normal to the band and the g_i are functions only of distance across the band, $\mathbf{n}\cdot\mathbf{x}$. Continuing equilibrium at the onset of localization requires that the traction-rate be continuous across the boundary of the band

$$n_i \Delta \dot{\sigma}_{ij} = 0 \tag{7}$$

If the constitutive relation is assumed to be the same inside and outside of the band at the inception of bifurcation, then use of (1a)–(1d) with (6) and (7) leads to a linear, homogeneous set of equations for the g_i (Rudnicki and Rice, 1975; Rice, 1976). Setting the determinant of the coefficient matrix equal to zero yields the condition on the band orientation and the constitutive parameters for which localization is possible. The magnitude of $\mathbf{g}$ is undetermined but the ratios of the components give the difference in the mode of deformation inside and outside of the band.

The Jaumann rate of stress that appears in (1a)–(1d), is related to the material rate in (7) by Prager (1961)

$$\hat{\sigma}_{ij} = \dot{\sigma}_{ij} - \Omega_{ik}\sigma_{kj} + \sigma_{ik}\Omega_{kj} \tag{8}$$

where the spin tensor $\mathbf{\Omega}$ is the anti-symmetric part of the velocity gradient tensor. Substituting (8) into (9) and using (6) yields

$$n_k \Delta \hat{\sigma}_{kj} = -\tfrac{1}{2}\{n_k g_k n_i \sigma_{ij} - g_k \sigma_{kj} + n_k \sigma_{kl} n_l g_j - n_k \sigma_{kl} g_l n_j\} \tag{9}$$

For an axially symmetric stress state, only σ_{33} and $\sigma_{11} = \sigma_{22}$ are nonzero. This simplifies expression (9) to

$$n_k \Delta \hat{\sigma}_{kj} = -\tfrac{1}{2}(\sigma_{33} - \sigma_{11})[n_3 n_\alpha g_\alpha - n^2 g_3] \tag{10a}$$

$$n_k \Delta \hat{\sigma}_{k\alpha} = -\tfrac{1}{2}(\sigma_{33} - \sigma_{11})[n_3^2 g_\alpha - n_\alpha n_3 g_3] \tag{10b}$$

where the subscript $\alpha = 1, 2$ and $n^2 = n_1^2 + n_2^2$. Inverting the constitutive relation (1a)–(1d), substituting into (10a) and (10b), and using (6) yields three homogeneous equations for g_1, g_2, and g_3:

$$(n_1 g_1 + n_2 g_2)\left[n_3\left(G_1^+ + \frac{9Kr}{4}\right)\right] + g_3\left[n^2 G_1^- + n_3^2\left(E + \frac{9Kvr}{2}\right)\right] = 0 \tag{11a}$$

$$\frac{9K}{4} n_2 (n_1 g_1 + n_2 g_2) + [n^2 G_t + n_3^2 G_1^+] g_2 + n_2 n_3 g_3 \left[G_1^- + \frac{9Kv}{2}\right] = 0 \tag{11b}$$

$$[n^2 G_t + n_3^2 G_1^+] g_1 + \frac{9K}{4} n_1 (n_1 g_1 + n_2 g_2) + n_1 n_3 g_3 \left[G_1^- + \frac{9Kv}{2}\right] = 0 \tag{11c}$$

The combinations $G_1^\pm = G_1 \pm (1/2)(\sigma_{33} - \sigma_{11})$ have been called slide moduli by Biot (1965). If the stress difference $(\sigma_{33} - \sigma_{11}) \ll G_1$, corresponding to neglecting the difference between the co-rotational and material stress rates in (1a)–(1d), these equations are identical to those given by Rudnicki (1977).

5. Compaction bands

The condition for a compaction band is easily determined from (11a)–(11c). Since the band normal is the direction of the maximum compressive stress, $n_3 = 1$, $n_1 = n_2 = 0$ (Fig. 3b). Thus, the only possibility for $g_3 \neq 0$ occurs when

$$E^{\mathrm{C}}_{\mathrm{crit}} = -9Krv/2 \tag{12}$$

The condition corresponds to a vanishing tangent modulus for the stress–strain curve for uniaxial strain ($D_{11} = D_{22} = 0$ in (1a)–(1d)). Compaction bands have been observed in axisymmetric compression tests

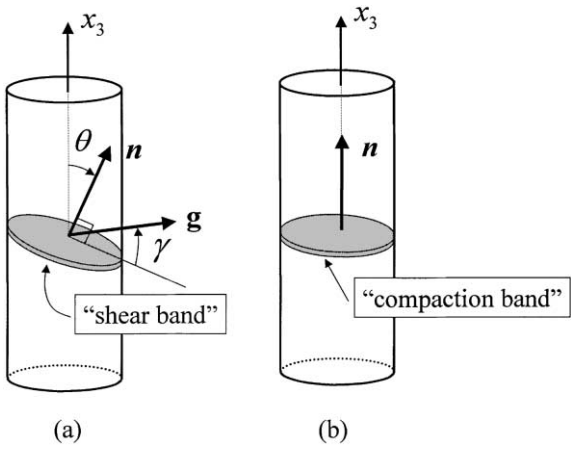

Fig. 3. Sketch of the localized zone geometry. (a) The normal to the plane of the band **n** makes an angle θ with the axial x_3 direction. The vector **g** makes an angle γ with the plane of the band. (b) For a compaction band **n** is in the x_3 direction and γ is in the opposite direction.

with constant lateral stress when the stress–strain curve is approximately flat, $E \approx 0$ and the condition (12) indicates that this requires at least one of r, v, or K to be zero. If $r = 0$, the axial deformation is not affected by increments of lateral compressive stress and for $r < 0$, compressive increments of lateral stress cause *compressive* axial deformation. If $v = 0$, axial deformation (at constant lateral confining stress) causes no lateral deformation; hence, the deformation is uniaxial compression. If $K = 0$, small increments of lateral compressive stress cause large increments of lateral deformation. This would be the case for very strong anisotropy caused by predominantly axial crack growth; the lateral stiffness would be reduced by opening of these cracks but this would require $v > 1/2$ and dilatant volumetric strain increments.

The condition (12) is similar to that obtained by Issen and Rudnicki (2000) in terms of the constitutive parameters used by Rudnicki and Rice (1975)

$$h^{\mathrm{C}}_{\mathrm{crit}} = -G_{\mathrm{e}} \frac{(1+\nu_{\mathrm{e}})}{3(1-\nu_{\mathrm{e}})} \left(1 + \frac{2\mu}{\sqrt{3}}\right)\left(1 + \frac{2\beta}{\sqrt{3}}\right) \tag{13}$$

An expression for the critical value of the tangent modulus in axisymmetric compression could be obtained by substituting $h^{\mathrm{C}}_{\mathrm{crit}}$ into (3a). Issen and Rudnicki (2000, 2001) note that the condition, $h^{\mathrm{C}}_{\mathrm{crit}} > 0$ requires one (but not both) of μ or β to be less than $-\sqrt{3}/2$. When $h/G_{\mathrm{e}} \ll 1$ in (3a)–(3d), the expressions (4) and (5) show that this corresponds to requiring that r or v (but not both) be less than zero. Issen and Rudnicki (2001) also note that the constitutive formulation of Rudnicki and Rice (1975) implicitly assumes that inelastic volumetric strain is due entirely to inelastic shear deformation, but, for very porous rocks, inelastic compaction also results from hydrostatic compression. Including this effect in an approximate way tends to reduce the effective value of ν_{e}. If the slope of the curve of hydrostatic compression versus inelastic volume strain becomes flat, the effective value of ν_{e} approaches -1 and, hence, $h^{\mathrm{C}}_{\mathrm{crit}}$ approaches zero.

Setting $n_3 = 1$, $n_1 = n_2 = 0$ in (11a) and (11b) reveals another possible mode of localized deformation with $g_3 = 0$ and either g_1 or g_2 nonzero. This occurs when

$$G_1^+ = 0 \tag{14}$$

which corresponds to the expression given by Rosen (1965) for the kinking stress to cause microbuckling of aligned-fibre composites. Budiansky and Fleck (1993) note that this expression overestimates the failure for conventional polymer matrix composites because microbuckling in these materials is primarily an inelastic

phenomenon rather than an elastic one, as assumed by Rosen (1965). The expression (14) may, however, be a more accurate estimate of the failure stress for open-cell materials, in which failure initiates by local shear buckling of a cell wall.

6. Shear bands

Shear bands also occurred in the experiments in which Olsson (1999) observed compaction bands and the analyses of Issen and Rudnicki (2000, 2001) suggest that small variations in material parameters may favor the appearance of either shear or compaction bands. Bésuelle (2001) has shown that the results of Rudnicki and Rice (1975) predict that the mode of deformation in the localized zone (shear versus dilation or compression) varies continuously between pure compaction and pure dilation. Consequently, it is useful to reexamine and expand upon the predictions of Rudnicki (1977) for shear band occurrence.

Setting the determinant of the coefficient matrix of the g_i in (11a) and (11b) equal to zero and solving for the tangent modulus E yields

$$E = -(9Krv/2) + \tan^2\theta\left\{\frac{(G_{\mathrm{l}}^{+} + 9Kr/4)(G_{\mathrm{l}}^{-} + 9Kv/4)}{G_{\mathrm{l}}^{+} + \tan^2\theta(G_{\mathrm{t}} + 9K/4)} - G_{\mathrm{l}}^{-}\right\} \tag{15}$$

where θ is the angle between the normal to the band and the axial (x_3) direction (Fig. 3a). If the difference between the Jaumann stress rate and the ordinary rate is neglected so that $G_{\mathrm{l}}^{+} = G_{\mathrm{l}}^{-} = G_{\mathrm{l}}$, then the angle giving the largest value of E satisfies

$$\tan^2\theta_{\mathrm{crit}} = \frac{\sqrt{(G_{\mathrm{l}} + 9Kr/4)(G_{\mathrm{l}} + 9Kv/4)} - G_{\mathrm{l}}}{(G_{\mathrm{t}} + 9K/4)} \tag{16}$$

Substituting (16) into (15) yields

$$E^{\mathrm{S}}_{\mathrm{crit}} = -2rv\left(\frac{9K}{4}\right) + \frac{\left[\sqrt{(G_{\mathrm{l}} + 9Kr/4)(G_{\mathrm{l}} + 9Kv/2)} - G_{\mathrm{l}}\right]^2}{(G_{\mathrm{t}} + 9K/4)} \tag{17}$$

Since the second term is positive (as long as $G_{\mathrm{t}} + 9K/4 > 0$), the critical tangent modulus for shear band onset exceeds that for compaction band onset, $E^{\mathrm{S}}_{\mathrm{crit}} > E^{\mathrm{C}}_{\mathrm{crit}}$. Thus, in a range where both compaction bands and shear bands are possible, the onset of shear bands will precede that of compaction bands if the tangent modulus is monotonically decreasing. The tangent modulus for axisymmetric deformation in porous rocks with constant lateral confining stress does not, however, appear to be monotonically decreasing (Zhang et al., 1990; Olsson, 1999). Typically, the modulus decreases to near zero or, possibly, even less than zero, remains near zero for an interval of strain and then increases again. The increase of the tangent modulus following the flat portion is evidently due to hardening associated with attainment of a more compacted structure throughout the specimen.

The angle between **g** and the plane of the band, denoted by γ (Fig. 3), is related to the band angle θ by

$$\tan\gamma = \frac{[G_{\mathrm{l}} - G_{\mathrm{t}} - (1-2v)(9K/4)]\sqrt{G_{\mathrm{l}} + 9Kr/4} - G_{\mathrm{l}}\sqrt{G_{\mathrm{l}} + 9Kv/2}}{\tan\theta_{\mathrm{crit}}(G_{\mathrm{t}} + 9K/4)\left[\sqrt{G_{\mathrm{l}} + 9Kr/4} + \sqrt{G_{\mathrm{l}} + 9Kv/2}\right]} \tag{18}$$

If normality is satisfied, $r = 2v$, the longitudinal shear modulus G_{l} does not appear in the expressions for the band angle and the critical tangent modulus. The band angle is given by

$$\tan^2\theta_{\mathrm{crit}} = \frac{r^2}{(1 + 4G_{\mathrm{t}}/9K)} \tag{19}$$

and the critical tangent modulus by

$$E^{\mathrm{S}}_{\mathrm{crit}} = \frac{-G_{\mathrm{t}} r^2}{(1 + 4G_{\mathrm{t}}/9K)} \tag{20}$$

Consistent with the predictions of Rudnicki and Rice (1975), the critical tangent modulus is always negative (to neglect of the co-rotational terms) when normality is satisfied.

If the shear moduli are negligible with respect to the transverse modulus, G_{l}, $G_{\mathrm{t}} \ll K$, the band angle is given by

$$\tan^2 \theta_{\mathrm{crit}} = \sqrt{2rv} \tag{21}$$

and the critical tangent modulus is

$$E_{\mathrm{crit}} = G_{\mathrm{l}} \left[\sqrt{2v} - \sqrt{r}\right]^2 - 2rvG_{\mathrm{t}} \tag{22}$$

(This expression corrects Eq. (17) of Rudnicki (1977) which is missing a factor of two in the third term.) Note that E_{crit} is always negative for normality, $r = 2v$, and increases if G_{t} is reduced relative to G_{l}. The expression (18) reduces to

$$\tan \gamma = -\left(\frac{r}{2v}\right)^{1/4} \frac{(1 - 2v)}{\sqrt{2v} + \sqrt{r}} \tag{23}$$

If the volume strain is compressional, v is less than $1/2$. In this case, γ is negative and the normal component of **g** is directed opposite to the band normal **n**.

These results are illustrated in Figs. 4–8. In each figure, results are plotted against values of v ranging from 0.01 (or, sometimes, 0.1) to 1. Recall that for axisymmetric compression the volumetric deformation is compactive (dilatant) for $v < (>)1/2$ and the lateral deformation is extensile (compressive) if $v > (<)0$. Because the band angle is easily observed in experiments, even when the precise onset of localization is difficult to determine, results are plotted in Figs. 4–6 for values of θ_{crit} equal to, 30°, 45°, 50°, 55° and 60°. Typical band angles for low porosity, dilatant rocks are around 60°, but Olsson (1999) observed shear bands at angles ranging from 14° to 43° in his experiments on Castlegate sandstone with a porosity 25–30%.

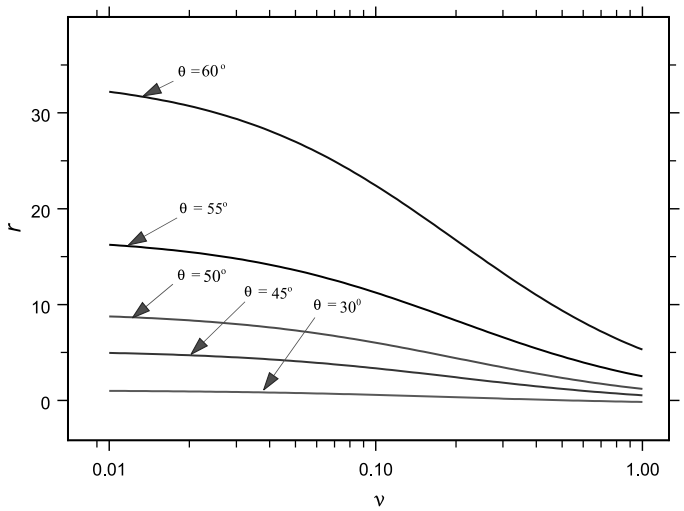

Fig. 4. Values of r and v satisfying (16) for different values of θ and $4G_{\mathrm{l}}/9K = 0.4$ and $4G_{\mathrm{t}}/9K = 0.1$.

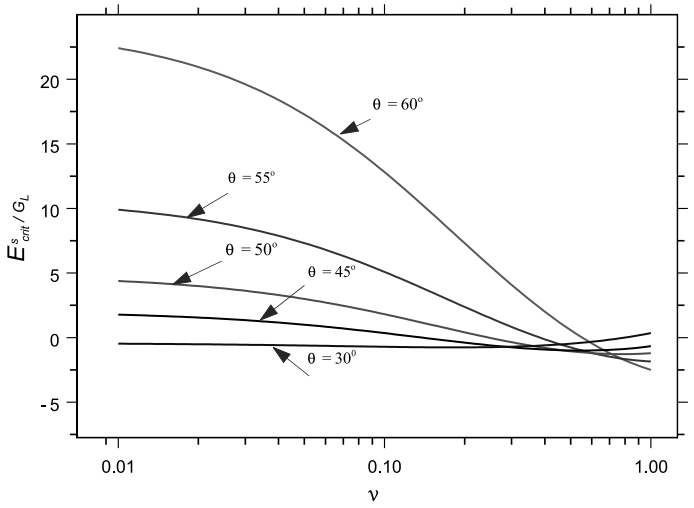

Fig. 5. Values of the critical tangent modulus at shear localization E^{S}_{crit} from (15) divided by G_l against ν for different values of θ and $4G_l/9K = 0.4$ and $4G_t/9K = 0.1$. Values of r are given in Fig. 4.

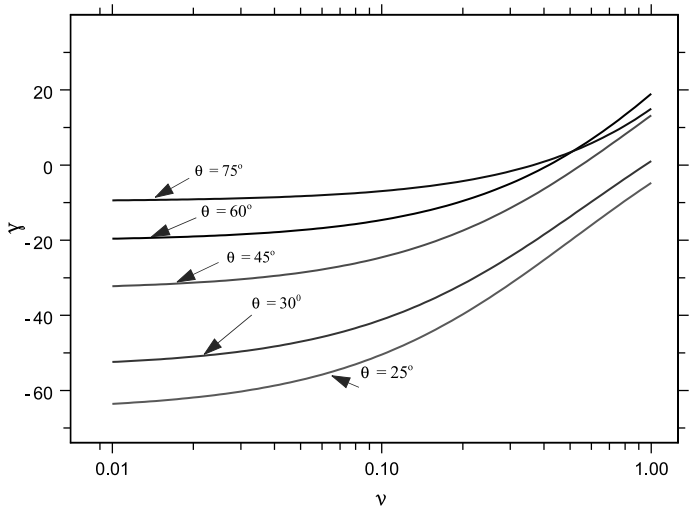

Fig. 6. Values of the mode angle γ from (18) versus ν for different values of θ and $4G_l/9K = 0.4$ and $4G_t/9K = 0.1$. Values of r are given in Fig. 4.

Bésuelle (2001) reported a systematic variation of angle in axisymmetric compression tests on Vosges sandstone, ranging from 54° at the lowest confining pressure, 10 MPa, down to 37° at 60 MPa. The decrease in angle with confining pressure is associated with a change in the volumetric deformation from dilation to compression. Fig. 4 shows the values of r satisfying (16) for $\overline{G}_l = 4G_l/9K = 0.4$ and $\overline{G}_t = 4G_t/9K = 0.1$. Fig. 4 shows that high angle shear bands require extremely large values of r unless ν is large (near unity or greater) corresponding to dilatant behavior. Low band angles are favored by small values of r or ν.

Fig. 5 shows the critical value of the tangent modulus E^{S}_{crit} divided by the longitudinal shear modulus G_l for the same parameters used in Fig. 4. Note that the value of r for each point in Fig. 5 is also determined

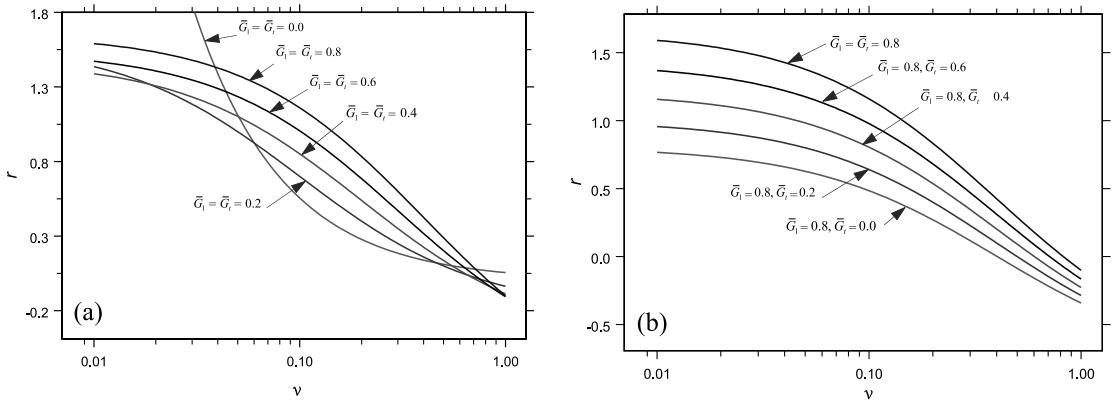

Fig. 7. Values of r and ν satisfying (16) for $\theta = 30°$ and various values of (a) $4G_l/9K = 4G_t/9K$ and (b) $4G_t/9K$ for $4G_l/9K = 0.8$.

from Fig. 4. For example, for $\nu = 0.1$ and $\theta = 60°$, Fig. 5 yields $E^S_{crit}/G_l \approx 12.5$, suggesting that a shear band would appear well before peak in the stress–strain curve and, perhaps, even near the elastic range. Fig. 4 shows, however, that for $\nu = 0.1$ and $\theta = 60°$, the value of r is very large, around 23, and probably far greater than is realistic. The graph does show that shear bands with angles of 30° can occur for $E^S_{crit} \approx 0$ for low values of ν corresponding to compactive behavior.

Fig. 6 shows the variation of the mode angle γ for the same values of $\overline{G}_l$ and $\overline{G}_t$ as in Figs. 4 and 5, 0.4 and 0.1, and a similar range of angles. (The same comment concerning the interpretation of Fig. 5 also applies here.) As expected, for smaller band angles and smaller values of ν, γ becomes more negative indicating a larger component of compactive strain normal to the band.

Figs. 7 and 8 show the effects of variations in the shear moduli $\overline{G}_l$ and $\overline{G}_t$ on the value of r required for a band angle of 30° (Fig. 7) and the corresponding ratio E^S_{crit}/G_l (Fig. 8). Figs. 7a and 8a show results for equal values of $\overline{G}_l$ and $\overline{G}_t$, 0.0 (omitted from Fig. 8a), 0.2, 0.4, 0.6 and 0.8. Figs. 7b and 8b show results for a fixed value of $\overline{G}_l = 0.8$ and $\overline{G}_t = 0.0$ (omitted from Fig. 8b), 0.2, 0.4, 0.6 and 0.8. Fig. 7a shows that the value of r for $\theta_{crit} = 30°$ increases with increasing $\overline{G}_l = \overline{G}_t$ for $0.08 \lesssim \nu \lesssim 0.8$. Outside this range, the dependence becomes more complicated and then reverses for much lower and higher values of ν. Increasing

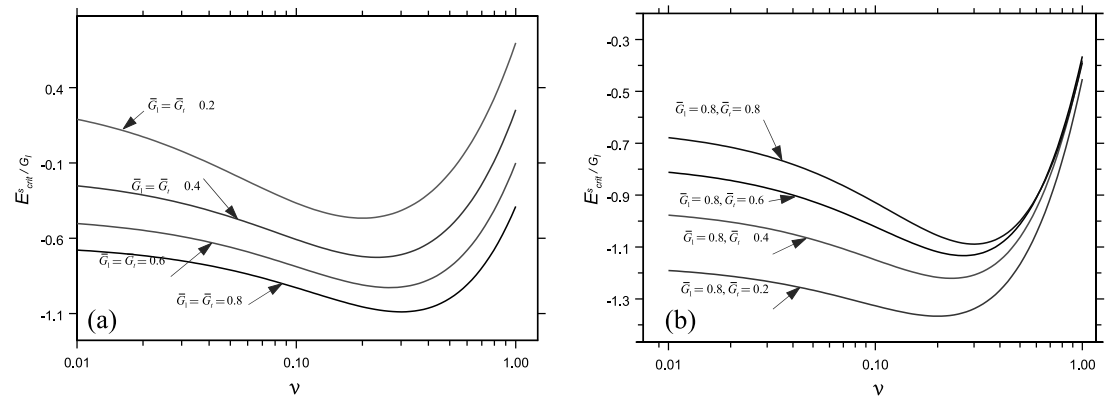

Fig. 8. Values of the critical tangent modulus at shear localization E^S_{crit} from (15) divided by G_l against ν for $\theta = 30°$ for various values of (a) $4G_l/9K = 4G_t/9K$ and (b) $4G_t/9K$ for $4G_l/9K = 0.8$.

$\overline{G}_l = \overline{G}_t$ decreases E^S_{crit}/G_l (Fig. 8a). Decreasing the ratio G_t/G_l from unity decreases the required value of r (Fig. 7b) and decreases (makes more negative) the corresponding value of E^S_{crit}.

7. Discussion

The predictions here treat the occurrence of a shear band or compaction band as a bifurcation from homogeneous deformation. This approach constrains the constitutive parameters for which bands of particular orientations can occur. The analysis predicts that formation of a compaction band is possible when the tangent modulus for uniaxial deformation vanishes. This requires that the tangent modulus for axisymmetric compression with constant lateral stress ($\hat{\sigma}_{11} = \hat{\sigma}_{22} = 0$) E satisfies (12). Olsson (1999) and Wong et al. (2001) observed compaction bands to form on flat portions of the stress–strain curve where $E^C_{crit} \approx 0$. Since the confining stress was constant in these experiments, (12) indicates that one of v, r, and K is zero. Fig. 6 of Olsson (1999) shows that the lateral strain measured at the mid-height of the specimen is roughly constant during the flat portion of the stress–strain curve suggesting that the deformation is one-dimensional corresponding to $v = 0$ (although it is not required by the boundary conditions to be so). The values of β inferred by Olsson (1999) and by Wong et al. (2001) imply, however, that $v > 0$. Whether this is due to uncertainty in their determination, the failure of the constitutive relation (2) to include anisotropy or inadequacy of the bifurcation approach to localization is unclear.

The analysis here pertains to the inception of compaction band formation. Recent experiments suggest, however, that much of what happens during the flat portion of the stress–strain curve may be due to band propagation or thickening or the formation of multiple bands. In this case, the flat portion of the apparent stress–strain curve does not indicate material response but instead the averaged response of inhomogeneous deformation. From acoustic emission measurements, Olsson and Holcomb (2000) infer that once local bands of compaction form they thicken with increasing boundary displacement until the entire specimen is compacted. They found that the boundary between the compacted and uncompacted regions propagated as a planar front with a speed roughly an order of magnitude greater than the imposed platen displacement rate. A kinematic analysis by Olsson (2001) that treats the compaction front as discontinuity in porosity propagating quasi-statically at constant stress shows that the propagation velocity is proportional to the platen velocity and to the reciprocal of the porosity jump. But the relation of propagation to other features of the constitutive response of the compacted and uncompacted material is unknown. Microscopic observations by DiGiovanni et al. (2000) indicated that the porosity decrease across this front was due to intense grain breakage and rotation. Olsson (2001) suggests that the incipient formation of the band is associated with a small drop in stress that precedes that flat portion of the nominal stress–strain curve. This would be consistent with the negative value of E^C_{crit} (12) predicted for positive values of r, v, and K. Also, Wong et al. (2001) note that the overall stress–strain curves for samples of Bentheim sandstone in which compaction bands were observed were hardening but "punctuated by episodic stress drops". They report that the number of compaction bands increased with the number of stress drops, a phenomenon similar to that observed in crushing of honeycombs (Papka and Kyriakides, 1998, 1999).

The analysis here is phrased in terms of the macroscopic, phenomenological constitutive properties and only indirectly related to the micromechanisms of deformation. In their field observations, Mollema and Antonellini (1996) observed compaction bands in sedimentary layers with high porosity (20–25%) and large grain sizes (0.3–0.8 mm) but deformation bands (involving both shear and dilation or compaction) in layers with lower porosity and smaller grain sizes. Higher porosity is probably reflected in smaller values of v but the correlation is, at best, indirect. DiGiovanni et al. (2000) compare the micromechanical deformation mechanisms of the Castlegate sandstone, in which Olsson (1999) observed compaction bands, with those of Berea sandstone, in which compaction bands have not been observed (Menéndez et al., 1996). Menéndez et al. (1996) found that compaction in Berea sandstone was primarily associated by the onset of brittle

microcracking at grain contacts, whereas DiGiovanni et al. (2000) found that grain breakage and fragmentation in the Castlegate sandstone was preceded by volume reduction due to breakage of grain contacts and rotation without fragmentation. They attribute the difference to fabric and cementation. Further work is needed to establish the relationship between microstructural features and the macroscopic response.

The macroscopic constitutive formulation used here also involves considerable uncertainty. The boundary of the stress states for which the response is elastic is depicted in Fig. 2 as a single surface. But constitutive formulations for porous rocks and granular materials often describe the behavior in terms of two surfaces: a shear yield (or failure) surface for which $\mu > 0$ and a "cap" (often assumed to be elliptical) intersecting the mean stress axis (Dimaggio and Sandler, 1971; Fossum and Fredrich, 2000). Issen (in press) has pointed out that the use of two surfaces is consistent with the likely predominance of different microscale deformation mechanisms at low (microcracking with dilatancy) and high mean stresses (pore collapse and grain crushing with compaction). Indeed, Wong et al. (2001) report that their observations rule out a constitutive model that does not include multiple deformation mechanisms. Conditions for localization near the intersection of the two surfaces are complicated but, by examining some special cases of a two surface model, Issen (in press) has shown that it is possible to choose parameters consistent with the range in which Olsson (1999) observed compaction bands.

Predictions of shear band formation are complicated by uncertainty about the shear moduli G_l and G_t which do not appear in the expression for the critical tangent modulus for a compaction band (12). The parameters r, v and K can be measured easily in the conventional axisymmetric compression geometry (although, in practice, the lateral confining pressure is kept constant) but G_l and G_t cannot. Nevertheless, observation of the angle that the band normal makes with the axis of the specimen is straightforward. Values less than 45° in compacting rocks (Olsson, 1999; Bésuelle, 2001) are consistent with predictions for low values of v (less than $1/2$). Comparison of predictions and observations of the critical tangent modulus is more difficult. The value at the onset of band formation is often difficult to determine precisely and the predicted value depends on the current values of the other constitutive parameters, which typically evolve with deformation. In addition, as discussed by Rudnicki and Rice (1975), the bifurcation analysis with a smooth yield surface constitutive formulation tends to predict excessively negative values of the tangent modulus for the onset of localization in axisymmetric compression. Because the kinematic condition (6) requires the difference between the localized field and the homogeneous field to be a plane-strain deformation (Rice, 1976; Bésuelle, 2001), the onset of localized deformation from an axisymmetric state requires an abrupt change in the deformation pattern. A smooth yield surface formulation is well known to overpredict the stiffness of response to such a change resulting in the prediction of an overly negative tangent modulus. This feature may, however, be a less significant factor for low angle shear bands involving a relatively large ratio of compaction to shear and, consequently, for which the deformation pattern is more similar to axisymmetric compression.

8. Conclusions

Predicted conditions for the onset shear bands and compaction bands in a transversely isotropic material are roughly in accord with observations. Small values v ($v \ll 1/2$) favor formation of compaction bands and of low angle shear bands (with normals $<45°$ from the symmetry axis) at near zero (or, even positive, in the case of shear bands) values of the tangent modulus. The condition $v = 0$ corresponds to uniaxial (one-dimensional) deformation. Because uniaxial strain is thought to approximate accurately the deformation state in many hydrocarbon reservoirs (eg., Teufel et al., 1991), nonuniform, localized compaction may be widespread. The detailed constitutive information needed for precise predictions is, however, not available. A particular need is for a better understanding of the transition from the regime of mean (compressive) stress that inhibits inelastic deformation to that which enhances it and how this transition is related to the

microstructural features such as cement, pore shape and fabric. In addition, accurate predictions of the tangent modulus at the onset of shear band formation require knowledge of the longitudinal and transverse shear moduli which cannot be measured directly in the axisymmetric compression configuration. Recent experimental work has suggested that the occurrence of compaction bands can be followed by propagation, or thickening of the compacted region of lower permeability.

Acknowledgements

I am grateful to Teng-fong Wong for suggesting that I re-examine the transversely isotropic constitutive relation for the possibility of compaction bands and to David Holcomb, Kathleen Issen and Bill Olsson for many helpful discussions on compaction bands. Partial financial support for this work was provided by US Department of Energy, Office of Basic Energy Sciences, Geosciences Research Program, through Grant DE-FG-02-93ER14344 to Northwestern University.

References

Batdorf, S.B., Budiansky, B., 1949. A mathematical theory of plasticity based on the concept of slip. Technical Note 1971, NACA, 33 pp.

Bésuelle, P., 2001. Compacting and dilating shear bonds in porous rock: theoretical and experimental conditions. Journal of Geophysical Research 106 (B7), 13435–13442.

Biot, M.A., 1965. Mechanics of Incremental Deformations. John Wiley and Sons, New York.

Bonner, B.P., 1974. Shear wave birefringence in dilating granite. Geophysical Research Letters 1 (5), 217–220.

Budiansky, B., Fleck, N.A., 1993. Compressive failure of fibre composites. Journal of the Mechanics and Physics of Solids 41 (1), 183–211.

Chau, K.T., 1992. Non-normality and bifurcation in a compressible pressure-sensitive circular cylinder under axisymmetric tension and compression. International Journal of Solids and Structures 29 (7), 801–824.

Chau, K.T., 1993. Antisymmetric bifurcations in a compressible pressure-sensitive circular cylinder under axisymmetric tension and compression. Journal of Applied Mechanics 60, 282–289.

Costin, L.S., 1983a. A microcrack damage model for brittle rock. Tech. Rep. SAND83-1590. Sandia National Laboratories, Albuquerque, NMexico.

Costin, L.S., 1983b. A microcrack model for the deformation and failure of brittle rock. Journal of Geophysical Research 88, 9485–9492.

Desrues, J., 2002. Shear band analysis and shear moduli calibration. International Journal of Solids and Structures 39, 3757–3776.

DiGiovanni, A.A., Fredrich, J.T., Holcomb, D.J., Olsson, W.A., 2000. Micromechanics of compaction in an analogue reservoir sandstone. In: Girard, J., Liebman, M., Breeds, C., Doe, T. (Eds.), Pacific Rocks 2000, Proceedings of the Fourth North American Rock Mechanics Symposium. A.A. Balkema, Rotterdam, pp. 1153–1158.

Dimaggio, F.L., Sandler, I.S., 1971. Material model for granular soils. Journal of Engineering Mechanics Division ASCE 97, 935–950.

Fossum, A.F., Fredrich, J.T., 2000. Cap plasticity models and compactive and dilatant pre-failure deformation. In: Proceedings of the Fourth North American Rock Mechanics Symposium, pp. 1169–1176.

Gioia, G., Cuitiño, A.M., 2001. Two-phase densification of cohesive granular aggregates. Preprint.

Hill, R., 1967. The essential structure of constitutive laws for metal composites and polycrystals. Journal of the Mechanics and Physics of Solids 15, 79–95.

Hoenig, A., 1979. Elastic moduli of a non-randomly cracked body. International Journal of Solids and Structures 15, 137–154.

Holcomb, D.J., Olsson, W.A., 2001. Compaction localization and fluid flow. Journal of Geophysical Research, submitted for publication.

Holcomb, D.J., Rudnicki, J.W., 2001. Inelastic constitutive properties and shear localization in Tennessee marble. International Journal for Numerical and Analytical Methods in Geomechanics 25, 109–129.

Hutchinson, J.W., 1970. Elastic–plastic behavior of polycrystalline metals and composites. Proceedings of the Royal Society of London A 319, 247–272.

Hutchinson, J.W., Miles, J.P., 1974. Bifurcation analysis of the onset of necking in an elastic/plastic cylinder under uniaxial tension. Journal of the Mechanics and Physics of Solids 22, 67–71.

Issen, K.A., 2002. The influence of constitutive models on localization conditions for porous rock. Engineering Fracture Mechanics, in press.

Issen, K.A., Rudnicki, J.W., 2000. Conditions for compaction bands in porous rock. Journal of Geophysical Research 105, 21529–21536.

Issen, K.A., Rudnicki, J.W., 2001. Theory of compaction bands in porous rock. Physics and Chemistry of the Earth 26 (1–2), 95–100.

Menéndez, B., Zhu, W., Wong, T.-F., 1996. Micromechanics of brittle faulting and cataclastic flow in Berea sandstone. Journal of Structural Geology 18 (1), 1–16.

Miles, J.P., Nuwayhid, U.A., 1985. Bifurcation in compressible elastic/plastic cylinders under uniaxial tension. Applied Scientific Research 42, 33–54.

Mollema, P., Antonellini, M.A., 1996. Compaction bands: a structural analog for anti-mode I cracks in aeolian sandstone. Tectonophysics 267, 209–228.

Olsson, W.A., 1992. The formation of a yield-surface vertex in rock. In: Tillerson, J.R., Wawersik, W.R. (Eds.), Proceedings of the 33rd US Symposium on Rock Rechanics. A.A. Balkema, Rotterdam, pp. 701–705.

Olsson, W.A., 1995. Development of anisotropy in the incremental shear moduli for rock undergoing inelastic deformation. Mechanics of Materials 21, 231–242.

Olsson, W.A., 1999. Theoretical and experimental investigation of compaction bands. Journal of Geophysical Research 104, 7219–7228.

Olsson, W.A., 2001. Quasistatic propagation of compaction fronts in porous rocks. Mechanics of Materials 33, 659–668.

Olsson, W.A., Holcomb, D.J., 2000. Compaction localization in porous rock. Geophysical Research Letters 27 (21), 3537–3540.

Ottosen, N.S., Runesson, K., 1991. Properties of discontinuous bifurcation solutions in elasto-plasticity. International Journal of Solids and Structures 27, 401–421.

Papka, S.D., Kyriakides, S., 1998. Experiments and full-scale numerical simulations of in-plane crushing of a honeycomb. Acta Metallurgica 46, 2765–2776.

Papka, S.D., Kyriakides, S., 1999. Biaxial crushing of honeycombs—part I: experiments. International Journal of Solids and Structures 36, 4367–4396.

Perrin, G., Leblond, J.B., 1993. Rudnicki and Rice's analysis of strain localization revisited. Journal of Applied Mechanics 60, 842–846.

Prager, W., 1961. Introduction to the Mechanics of Continua. Ginn and Company, Boston (reprinted by Dover, 1973).

Rice, J., 1976. The localization of plastic deformation. In: Koiter, W. (Ed.), Theoretical and Applied Mechanics. 14th IUTAM Congress. North-Holland, Amsterdam, pp. 207–220.

Rosen, B.W., 1965. Fibre Composite Materials, Am. Soc. Metals Seminar. American Society of Metals (Chapter 3).

Rudnicki, J.W., 1977. The effect of stress-induced anisotropy on a model of brittle rock failure as localization of deformation. In: Wang, F.-D., Clark, G.B. (Eds.), Energy Resources and Excavation Technology. Proceedings of the 18th US Symposium on Rock Mechanics, Keystone, Colorado, 22–24 June, pp. 3B4-1–3B4-8.

Rudnicki, J.W., Chau, K.T., 1996. Multiaxial response of a microcrack constitutive model for brittle rock. In: Aubertin, M., Hassani, F., Mitri, H. (Eds.), Tools and Techniques in Rock Mechanics. Proceedings of NARMS'96, 2nd North American Rock Mechanics Symposium, ISRM Regional Conference, 19–21 June. A.A. Balkema, Rotterdam, pp. 1707–1714.

Rudnicki, J.W., Rice, J.R., 1975. Conditions for the localization of deformation in pressure-sensitive dilatant materials. Journal of the Mechanics and Physics of Solids 23, 371–394.

Sulem, J., Vardoulakis, I., Papamichos, E., Oulahna, A., Tronvall, J., 1999. Elasto-plastic modelling of Red Wildmoor sandstone. Mechanics of Cohesive-Frictional Materials 4 (3), 215–245.

Teufel, L.W., Rhett, D.W., Farrell, H.E., 1991. Effect of reservoir depletion and pore pressure drawdown on in situ stress and deformation in the Ekofisk Field, North Sea. In: Proceedings of the 32nd US Symposium on Rock Mechanics. A.A. Balkema, Rotterdam, pp. 63–72.

Vardoulakis, I., Graf, B., 1985. Calibration of constitutive models for granular materials using data from biaxial experiments. Géotechnique 35, 299–317.

Wawersik, W.R., Rudnicki, J.W., Dove, P., Harris, J., Logan, J.M., Pyrak-Nolte, L., Orr Jr., F.M., Ortoleva, P.J., Richter, F., Warpinski, N.R., Wilson, J.L., Wong, T.-F., 2001. Terrestrial sequestration of CO_2: an assessment of research needs. In: Dmowska, R. (Ed.), Advances in Geophysics, vol. 43. Academic Press, New York, pp. 97–177.

Wong, T.-F., Baud, P., Klein, E., 2001. Localized failure modes in a compactant porous rock. Geophysical Research Letters 28 (13), 2521–2524.

Wong, T.-F., Gu, Y., Yanagidani, T., Zhao, Y., 1992. Stabilization of faulting by cumulative slip. In: Evans, B., Wong, T.-F. (Eds.), Fault Mechanics and Transport Properties of Rocks. Academic Press Limited, New York.

Zhang, J., Wong, T.-F., Davis, D.M., 1990. Micromechanics of pressure-induced grain crushing in porous rock. Journal of Geophysical Research 95, 341–352.